ELSEVIER

Journal of Nuclear Materials 312 (2003) 224–235

journal of nuclear materials

www.elsevier.com/locate/jnucmat

Densification behaviour of ThO_2–PuO_2 pellets with varying PuO_2 content using dilatometry

T.R.G. Kutty [a,*], P.V. Hegde [a], J. Banerjee [a], K.B. Khan [a], A.K. Sengupta [a], G.C. Jain [a], S. Majumdar [a], H.S. Kamath [b]

[a] *Radiometallurgy Division, Bhabha Atomic Research Centre, Trombay, Mumbai 400 085, India*
[b] *Nuclear Fuels Group, Bhabha Atomic Research Centre, Trombay, Mumbai 400 085, India*

Received 3 June 2002; accepted 21 November 2002

Abstract

The shrinkage behaviour of ThO_2, ThO_2–30%PuO_2, ThO_2–50%PuO_2 and ThO_2–75%PuO_2 pellets has been studied using a dilatometer in inert (Ar) and reducing atmospheres (Ar–8%H_2). The effects of dopants of CaO and Nb_2O_5 on shrinkage of the oxides of the above Pu/(Pu + Th) ratios were also studied. Out of the two dopants studied, CaO was found to give larger shrinkage for all the Pu/(Pu + Th) ratios covered in this study. It was also found that the shrinkage was marginally larger in Ar–8%H_2 than in Ar atmosphere. Addition of PuO_2 to ThO_2 enhanced sintering. This was found to be true for both the dopants. During the sintering of ThO_2, a prominent peak was observed in the shrinkage curve at around 100–300 °C. This peak was attributed to the pressure increase of the trapped gases which subsequently release at high temperatures.

PACS: 81.20.Ev; 61.72.−y; 66.30.Fq

1. Introduction

The proliferation potential of the light water reactor fuel in the fuel cycle may be significantly reduced by the utilization of thorium as a fertile component of the nuclear fuel [1]. The main benefits of the thorium cycle concept include (a) high actinide burnup, (b) inherent proliferation resistance, (c) improved radiation stability due to low fuel temperatures, (d) low volume of waste generation, (e) low fabrication cost and (f) low fuel failure rate [2,3]. ThO_2 has a higher melting point, better radiation stability, higher resistance to chemical interactions, lower vapour pressure and higher thermal conductivity than UO_2 [4,5]. The long-lived minor actinides resulting from fission are generated in much lower quantity with the thorium cycle, especially compared with the plutonium cycle. This ecological advantage is an important argument brought forward these days. The above-mentioned properties suggest that thorium based fuels have a greater potential safety and fuel durability than the currently used UO_2 or mixed oxide fuels (MOX). Several reactor concepts based on the thorium fuel cycle are under consideration since thorium is much more abundant than uranium. Today MOX (U, Pu) fuels are used in some conventional reactors, with ^{239}Pu providing the main fissile ingredient. An alternative is to use Th/Pu fuels with plutonium being consumed and fissile ^{233}U being bred [6–8]. In the energy amplifiers, Th–Pu mixtures [4] are being considered as the candidate fuel which is more effective in eliminating plutonium at acceptable concentrations than the conventional mixture of uranium and plutonium. The device operates as an effective thorium converter to ^{233}U. The latter can

* Corresponding author. Tel.: +91-22 559 2466/5361; fax: +91-22 550 5151.
E-mail address: tkutty@magnum.barc.ernet.in (T.R.G. Kutty).

0022-3115/03/$ - see front matter
PII: S0022-3115(02)01643-4

be subsequently mixed with ordinary or depleted uranium and it constitutes excellent fuels for PWRs.

The main motivations for considering ThO_2 as a matrix for burning plutonium (weapons or reactor grade) in conventional reactors are [9,10]:

1. Very little plutonium is produced from the irradiation of the matrix (in contrast to MOX fuel).
2. The amount of ThO_2 the core can handle is not limited by the Doppler effect considerations as is the case with inert matrices.
3. The reactivity of the ThO_2 matrix containing plutonium should be approximately constant since the reactivity decrease by plutonium burning should be balanced by a reactivity increase through the generation of ^{233}U. This raises the possibility of very long irradiation times of the fuel in the reactor and the associated deep burning of the plutonium.

Very few reports are available on the ThO_2–PuO_2 system. Therefore, a study was undertaken to have an in-depth knowledge about some of the properties of ThO_2–PuO_2 pellets. In this work, the shrinkage behaviour of ThO_2, ThO_2–30%PuO_2, ThO_2–50%PuO_2 and ThO_2–75%PuO_2 pellets was studied using a dilatometer in inert (Ar) and reducing atmospheres (Ar–8%H_2). The effects of CaO and Nb_2O_5 dopants on shrinkage behaviour of the pellets of the above $Pu/(Pu + Th)$ ratios are also evaluated. So far, studies have not been made on above-mentioned metal ratios in atmospheres like Ar and Ar–8%H_2. The results of this study would be useful to the manufacturers of such fuels.

2. Th–Pu–O system

Freshley and Mattys [11,12] have shown that ThO_2 and PuO_2 form a complete solid solution in the whole composition range like ThO_2 and UO_2. The lattice parameter of fluorite type cubic phase was found to decrease regularly from 0.5597 nm for ThO_2 to 0.5396 nm for pure PuO_2 [13]. Due to the limited amount of experimental data a more accurate assessment of the phase diagram is not yet possible. However, a few data exist of the phase diagram of this system [14]. The melting point of the ThO_2–PuO_2 solid solutions, containing various amounts of PuO_2, was measured in He. The melting point of the specimens containing less than 25%ThO_2 was found to be unchanged. A continuous series of solid solution has been reported by Mulford and Ellinger [15]. They found only a single fluorite structure by X-ray diffraction (XRD) and also showed that the lattice parameter varied linearly with composition. Dawson [16] has made magnetic susceptibility measurements on PuO_2 and ThO_2 mixtures and implied that solid solution following Vegard's law exists.

ThO_2 is the only stable solid oxide in the thorium–oxygen system and it has very little non-stoichiometry compared with UO_2. Its crystal structure is a cubic fluorite type, isomorphous with UO_2, PuO_2 and CeO_2 containing four thorium atoms and eight oxygen atoms in the unit cell. Th^{4+} is the only one stable valence state of thorium [17]. It can therefore be used as a model oxide if the deviations from the stoichiometry are to be avoided. On the other hand, the phase diagram of the plutonium–oxygen system shows the presence of four compounds namely Pu_2O_3, $PuO_{1.52}$, $PuO_{1.61}$ and PuO_2. PuO_2 is the most stable oxide of plutonium [18–21]. The lattice dimension and density of PuO_2 are 0.5396 nm and 11.46 g/cm^3, respectively. PuO_2 loses oxygen readily at elevated temperatures in either vacuum, reducing or inert atmospheres. This deviation from stoichiometry is accompanied by the formation of oxygen vacancies on the oxygen ion sublattice of the crystal [22,23]. This oxygen deficiency results in the formation of larger Pu^{3+} ions, which causes the unit cell to expand [24]. Unlike UO_2, PuO_2 does not readily incorporate excess oxygen in the interstitial sites and therefore PuO_{2+x} formation has not been reported. PuO_2 can combine with oxygen by adsorption on the surface. The amount of the adsorbed oxygen is proportional to the surface area [25].

3. Experimental

3.1. Fabrication of green pellet

The fabrication process for thorium based fuels is similar to that of UO_2. The green ThO_2 pellets and ThO_2–PuO_2 pellets for this study were prepared by the conventional powder metallurgy technique which consists of the following steps:

- milling of the as-received ThO_2 powder in a planetary ball for 8 h using tungsten carbide balls to break its platelet morphology;
- mixing/milling of the above milled ThO_2 powder with the required quantity of PuO_2 powder and additive (0.5 wt%CaO or 0.25 wt%Nb_2O_5) for 4 h in a planetary ball mill with tungsten carbide balls;
- double pre-compaction at 150 MPa;
- granulation of the pre-compacts;
- final cold compaction of the granulated powder at 300 MPa into green pellets.

The concentrations of the dopants to be added depend on its effectiveness in creating defects. They should be added as bare minimum quantities to reduce the amount of impurities in the sintered pellets. The study conducted by authors' laboratory on ThO_2 has shown that best optimum properties (like density, grain size, etc.) are obtained with 0.25 wt% Nb_2O_5 and 0.5 wt%

CaO. Hence we have adopted these concentrations. Depending upon the composition, the density of the green compacts was found to vary between 55% and 67% of the theoretical density. To facilitate compaction and to impart handling strength to the green pellets, 1 wt% zinc behenate was added as lubricant/binder during the last 1 h of the mixing/milling procedure. The green pellets were about 4.6 mm in diameter and around 7 mm in length. The characteristics of the starting ThO_2 and PuO_2 powders used in this study are given in Table 1. Impurity contents of ThO_2 and PuO_2 powders before doping are shown in Table 2.

Table 1
Characteristics of ThO_2 and PuO_2 powders

Property	ThO_2	PuO_2
Oxygen to metal ratio	2.00	2.00
Apparent density (g/cm^3)	0.70	1.2
Total impurities (ppm)	<1200	<1200
Specific surface area (m^2/g)	1.53	13.6
Theoretical density (g/cm^3)	10.00	11.46

Table 2
Metallic impurities in ThO_2 and PuO_2 powders before the addition of additives

Impurity (ppm)	ThO_2	PuO_2
Na	<50	<50
Ca	<100	<120
Al	<10	<10
Mg	<20	<25
Si	<70	<100
Fe	<120	<150
Cr	<70	<60
Co	<5	<5
Ni	<70	<60
Mo	<5	<5
W	<60	<50
B	<0.18	<0.18

3.2. Dilatometry

The shrinkage behaviour of ThO_2, ThO_2–30%PuO_2, ThO_2–50%PuO_2 and ThO_2–75%PuO_2 compacts in the various atmospheres was studied using a push rod type dilatometer (Netzsch, Model 402E7). The shrinkage was measured in axial direction. The sample supporter, measuring unit and displaceable furnace of the dilatometer were mounted horizontally as shown in Fig. 1. The length change measurements were made by a linear voltage differential transducer (LVDT) which was maintained at a constant temperature by means of water circulation from a constant temperature bath. The accuracy of the measurement of change in length was within ±0.1 μm. The temperature was measured using a calibrated thermocouple which is placed directly above the sample. A small force of 0.2 N was applied to the sample through the push rod. The dilatometric experiments were carried out in the gas flow of a rate 18 l/h. The impurity contents of the cover gases used in this study are given in Table 3.

The heating rate used for the above studies was 6 K/min. Length measurement was made in situ under dynamic condition. As the sample is heated, its temperature and length values are measured continuously with the help of a thermocouple and LVDT, respec-

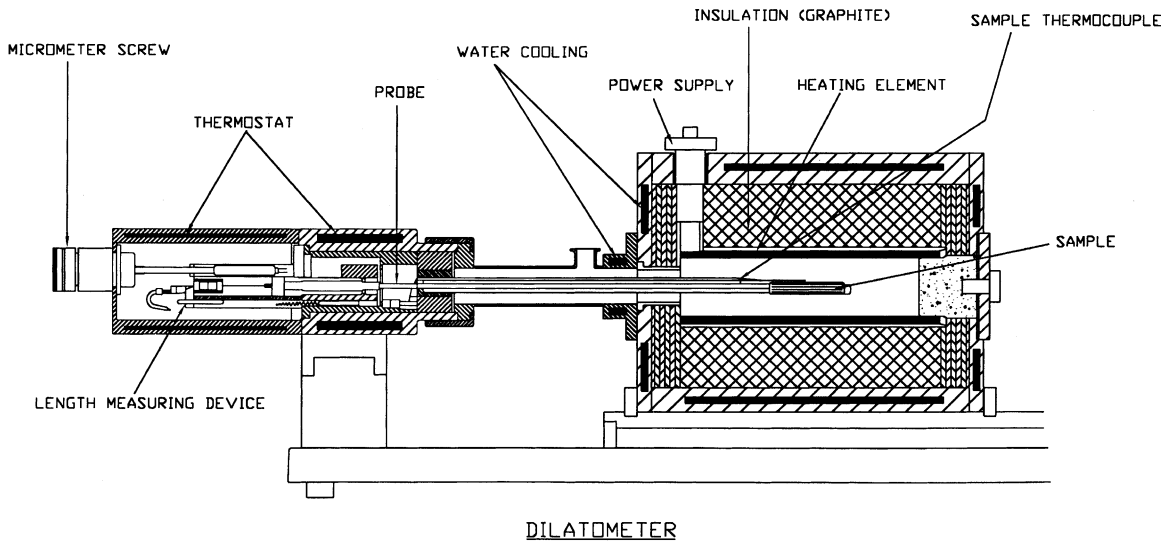

Fig. 1. A schematic of dilatometer showing sample, push rod, thermocouple, and LVDT probe.

Table 3
Impurity contents of different sintering atmospheres (volume ppm)

Sintering atmosphere	O_2 (vppm)	Moisture (vppm)	CO_2 (vppm)	CO (vppm)	N_2 (vppm)	Oxides of N_2 (vppm)	Hydrocarbon (vppm)
Ar	4	4	1	1	10	1	1.5
$Ar + 8\%H_2$	4	4	1	1	10	1	2

tively. The selection of the temperature programme was made by a computer via data acquisition system. The expansion of the system was corrected by taking a run under identical condition using a standard sample (POCO graphite, NIST).

3.3. Characterization

The mixed (Th, Pu) oxide pellets sintered in different atmospheres were characterized in terms of their density, oxygen to metal ratio (O/M) and phase content. The O/M ratio was measured thermogravimetrically and the phase content was estimated using X-ray diffractometry and metallography. Table 4 gives the typical values of O/M ratio and the density of the ThO_2–PuO_2 pellets. The XRD patterns of the pellets were obtained by using CuK_α radiation and graphite monochromator. For metallography, the sintered pellet was mounted in Bakelite and ground using successive grades of emery paper. The final polishing was done using diamond paste.

4. Results

The shrinkage behaviour of ThO_2 under Ar and Ar–$8\%H_2$ atmospheres are plotted in the form of percentage of shrinkage $[(dL/L_0) \times 100]$ versus temperature, where L_0 is the initial length. The result is shown in Fig. 2. The corresponding shrinkage rate $d(dL/L_0)/dt$ of the above pellet is shown in Fig. 3. Fig. 4 shows shrinkage behaviour of ThO_2–$30\%PuO_2$ pellets in Ar and Ar–$8\%H_2$. The corresponding shrinkage rate $(d(dL/L_0)/dt)$ is shown in Fig. 5. Figs. 6 and 7 illustrate the shrinkage of ThO_2–$50\%PuO_2$ and ThO_2–$75\%PuO_2$ pellets, respectively. Fig. 8 shows the intercomparison of the shrinkage curves for CaO doped pellets of ThO_2, ThO_2–$30\%PuO_2$, ThO_2–$50\%PuO_2$ and ThO_2–$75\%PuO_2$ in Ar–$8\%H_2$. Fig. 9 shows the shrinkage curves for the above samples of ThO_2 and ThO_2–PuO_2 in Ar atmosphere.

It can be seen from Fig. 2 that the onset of shrinkage occurs for ThO_2 at around 1200 °C in both Ar and Ar–$8\%H_2$. This is true for both CaO and Nb_2O_5 doped pellets. However, the shrinkage is larger for the pellets

Table 4
Typical values of green and sintered density, O/M ratio of ThO_2–PuO_2 pellets sintered in various atmospheres

Pellet composition	Dopant	Sintering vatmosphere	Green density (%TD)	Sintered density (%TD)	O/M ratio
ThO_2	CaO	Ar	67	93	2.000
		Ar–$8\%H_2$	67	95	2.000
	Nb_2O_5	Ar	67	96	2.000
		Ar–$8\%H_2$	67	96	2.000
ThO_2–$30\%PuO_2$	CaO	Ar	61	88	1.965
		Ar–$8\%H_2$	61	91	1.947
	Nb_2O_5	Ar	61.5	87	1.960
		Ar–$8\%H_2$	61.5	89	1.942
ThO_2–$50\%PuO_2$	CaO	Ar	58	89	1.934
		Ar–$8\%H_2$	58	90	1.921
	Nb_2O_5	Ar	58	87	1.930
		Ar–$8\%H_2$	58	88	1.924
ThO_2–$75\%PuO_2$	CaO	Ar	55	86	1.926
		Ar–$8\%H_2$	55	85	1.887
	Nb_2O_5	Ar	56	85	1.922
		Ar–$8\%H_2$	56	87	1.880

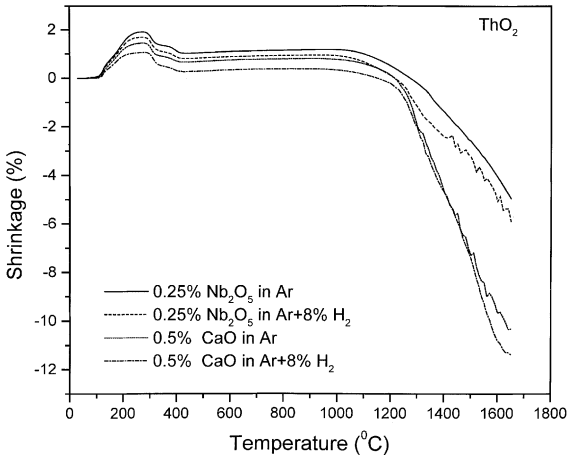

Fig. 2. Shrinkage curves for ThO_2 pellets in Ar–8%H_2 and Ar atmospheres. The percentage shrinkage ($dL/L_0 \times 100$) values are plotted against temperature, where L_0 is the initial length. The shrinkage curves are those with the dopants given in the figure.

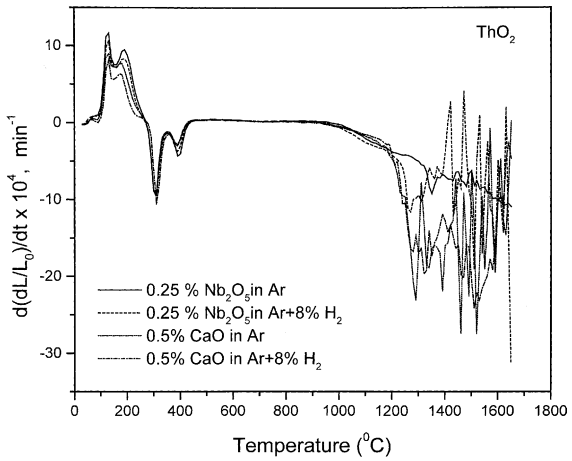

Fig. 3. Shrinkage rate $d(dL/L_0)/dt$ of ThO_2 pellet in Ar–8%H_2 and Ar atmospheres, for CaO and Nb_2O_5 dopants, plotted against temperature.

doped with CaO than those doped with Nb_2O_5 in both the sintering atmospheres. For example, at 1600 °C, the shrinkage for CaO doped ThO_2 pellet is about 11% in Ar–8%H_2 and that for Nb_2O_5 doped pellet in the same atmosphere is only 6%. It is also observed that amongst the two atmospheres, Ar–8%H_2 was found to give larger shrinkage for both the dopants.

At temperatures above 1200 °C, the shrinkage curve for ThO_2–30%PuO_2 pellet in Ar–8%H_2 lies just below that of Ar indicating a faster shrinkage in Ar–8%H_2 (Fig. 4). This is applicable for both the dopants covered in this study. The onset of shrinkage occurs at 1100 °C

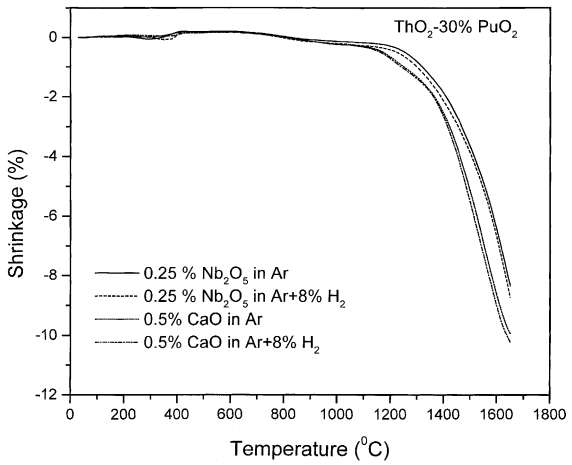

Fig. 4. Shrinkage curves for CaO and Nb_2O_5 doped ThO_2–30%PuO_2 pellets in Ar–8%H_2 and Ar atmospheres.

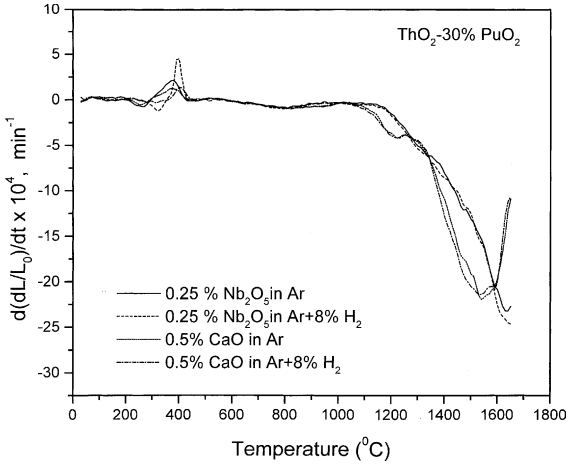

Fig. 5. Shrinkage rate for ThO_2–30%PuO_2 pellet in Ar–8%H_2 and Ar plotted against temperature for both the dopants of CaO and Nb_2O_5.

for CaO doped pellet, which is about 100 °C lower than that for the Nb_2O_5 doped pellet. For ThO_2–50%PuO_2, in the temperature ranges of 1100–1450 °C, the shrinkage is larger for Nb_2O_5 doped pellet (Fig. 6) than that for the CaO doped pellet.

It is noted from Fig. 7 that the shrinkage slows down in the temperature at around 900–1100 °C for ThO_2–75%PuO_2 pellet in Ar and Ar–8%H_2 atmospheres for both CaO and the Nb_2O_5 doped pellets. The slowing down of the shrinkage process was also noted for ThO_2–50%PuO_2 pellet to a lesser extent in the above temperature range.

For ThO_2 pellets, large oscillations were noticed in some cases above 1250 °C in $d(dL/L_0)/dt$ curves (see

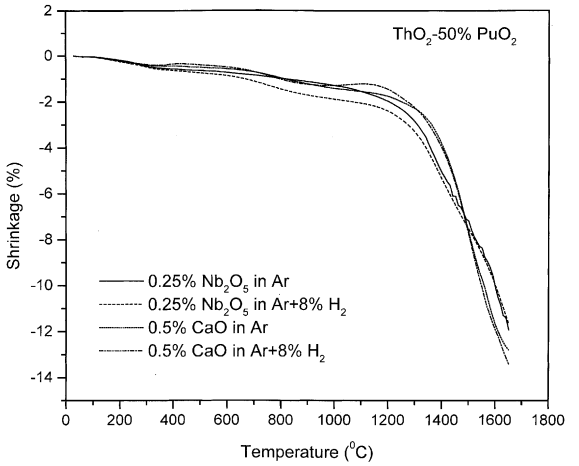

Fig. 6. Shrinkage curves for ThO_2–50%PuO_2 in Ar–8%H_2 and Ar atmospheres.

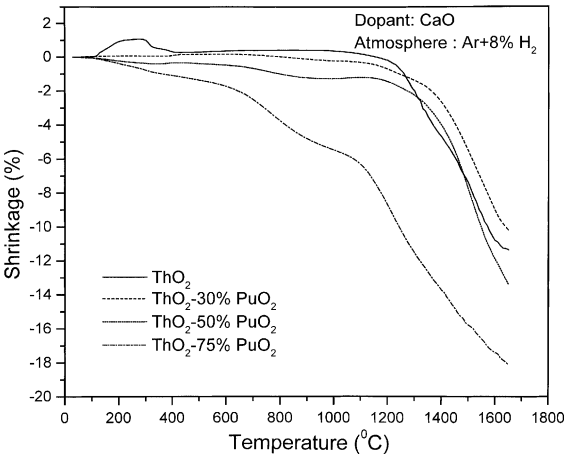

Fig. 8. Intercomparison of the shrinkage behaviour of CaO doped ThO_2, ThO_2–30%PuO_2, ThO_2–50%PuO_2 and ThO_2–75%PuO_2 in reducing atmosphere (Ar–8%H_2).

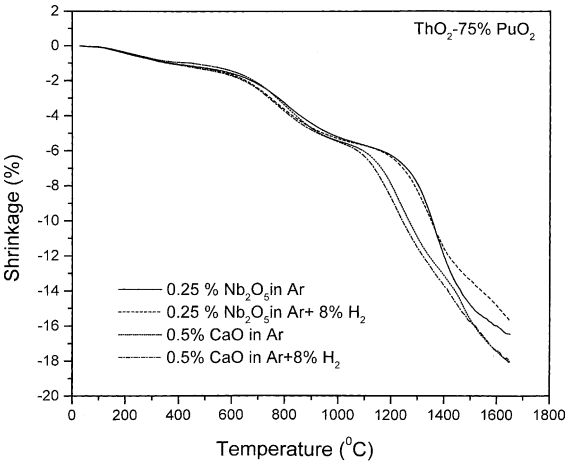

Fig. 7. Percentage shrinkage ($dL/L_0 \times 100$) values plotted against temperature for ThO_2–75%PuO_2 for different atmospheres and different dopants.

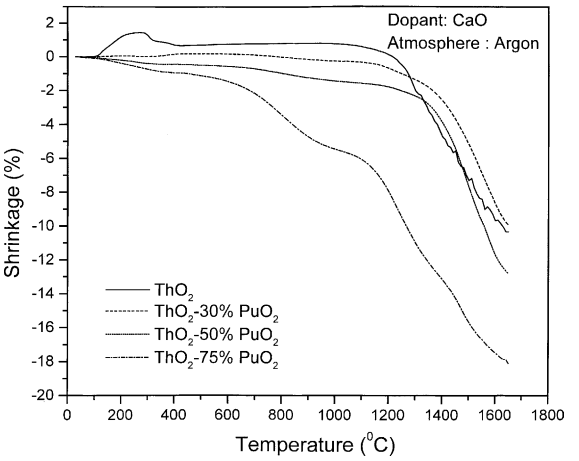

Fig. 9. Shrinkage curves of CaO doped, ThO_2, ThO_2–30%PuO_2, ThO_2–50%PuO_2 and ThO_2–75%PuO_2 in inert atmosphere (Ar).

Fig. 3). Similar observations have been noted for ThO_2–50%PuO_2 and ThO_2–75%PuO_2 pellets in small magnitude.

A prominent peak was observed in the shrinkage curve between 100 and 300 °C for ThO_2 pellet (see Fig. 2). This peak was present for all the ThO_2 runs carried out in both Ar and Ar–8%H_2 atmospheres. This peak was however absent for all samples containing plutonium.

The significant observations are summarized below:

1. CaO was found to give larger shrinkage than Nb_2O_5 in Ar and Ar–8%H_2 atmospheres for all the samples of ThO_2 and ThO_2–PuO_2.
2. Shrinkage was found to be marginally larger in Ar–8%H_2 atmosphere than in Ar.
3. Large oscillations were noticed in $d(dL/L_0)/dt$ curves of ThO_2 pellet.
4. A peak was noticed in the shrinkage curves of ThO_2 in the low temperature region of 100–300 °C.

The XRD patterns of ThO_2 and ThO_2–30%PuO_2 pellets sintered in both Ar and Ar–8%H_2 showed only a single phase. But the XRD patterns of the pellets with higher plutonium contents (such as ThO_2–50%PuO_2 and ThO_2–75%PuO_2 pellets) sintered in Ar and Ar–8%H_2 showed the presence of two phases. One is isostructural with PuO_2 (fluorite) and the other is isostructural with

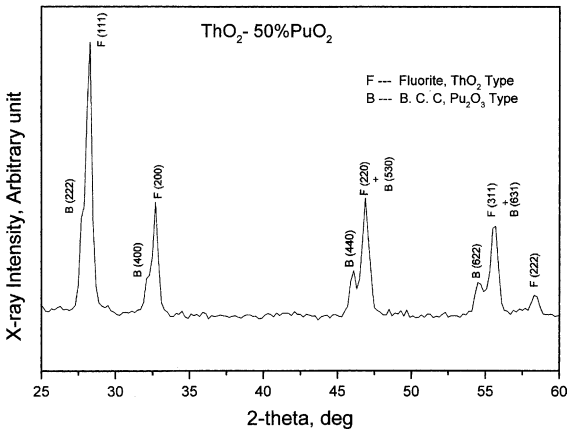

Fig. 10. XRD pattern of Nb_2O_5 doped ThO_2–50%PuO_2 pellet in Ar–8%H_2 showing the presence of two phases.

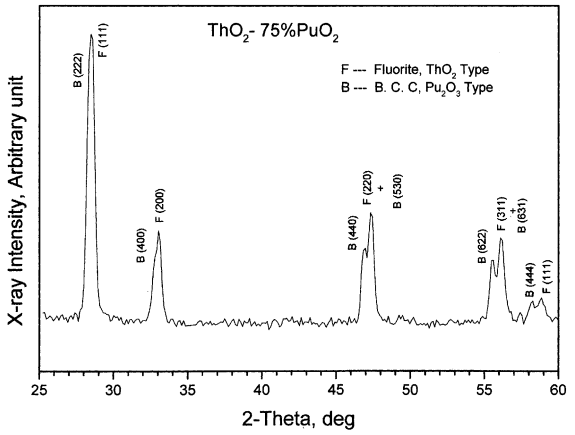

Fig. 11. XRD pattern of Nb_2O_5 doped ThO_2–75%PuO_2 pellet sintered in Ar–8%H_2 atmosphere.

bcc α-Pu_2O_3 (see Figs. 10 and 11). Some portion of PuO_2 has combined with ThO_2 to form a fluorite type solid solution and the rest of the PuO_2 might have been reduced to bcc α-Pu_2O_3 which combined with ThO_2 forming bcc α-Pu_2O_3 type solid solution.

5. Discussion

From the above results, it is evident that the shrinkage occurs more rapidly for CaO doped pellets in both the atmospheres. And also for the same dopant, the shrinkage increases with the increase of PuO_2 content. At 1300 °C, the shrinkage was negligible (<1%) for pure ThO_2 in Ar–8%H_2, but it was more than 11% for ThO_2–75%PuO_2 in the same atmosphere (see Fig. 8). It was also noticed for the same dopant (CaO) that Ar–8%H_2 is marginally better for sintering than Ar for all samples of ThO_2 and ThO_2–PuO_2 covered in this study.

The sinterability of ThO_2–PuO_2 compacts has been found to depend upon the following factors, namely [26,27]:

1. Sintering temperature.
2. Sintering atmosphere.
3. Characteristics of the starting ThO_2 and PuO_2 powders.
4. Sintering time.
5. Nature of the dopant/sintering aid.

Sintering is a diffusion controlled process and is rate controlled by the slower moving metal atoms. Diffusion in solid itself occurs by jumps on an atomic scale via the movement of point defects. The point defect model has been used to explain many observed features of diffusion in non-stoichiometric fluorite type oxide fuels [23].

5.1. Point defect model

The point defect model was first developed by Matzke [23,28] and Lidiard [29]. They derived a relation for the temperature dependence of the concentration of vacancies and interstitials in both the oxygen and metal sublattice by solving the anion Frenkel, Schottky and cation Frenkel products. It has been shown that the activation enthalpy for metal diffusion should increase or decrease by ΔG_{FO} when passing from MO_2 to MO_{2+x} or MO_{2-x}, respectively, if the metal diffusion occurs via a vacancy mechanism, where ΔG_{FO} is the free energy of formation of oxygen Frenkel defects [23].

The point defects are created in the materials by the following process:

1. Deviation from stoichiometry.
2. Addition of a dopant having valency that is different from that of the host metal ion.
3. Thermal activation, provided that the temperature is high enough.

In the hypostoichiometric region the fluorite type oxides have high concentrations of oxygen vacancies whereas in the hyperstoichiometric region they show high concentrations oxygen interstitials. The concentrations of metal defects are always low. To achieve mass transport in ThO_2 in the true sense, both thorium and oxygen atoms has to be transported. In ThO_2, the heavy thorium atom moves much slower than the light oxygen atom. Hence the rate controlling process will be the mobility of thorium atom. At higher concentrations, the defects will aggregate into clusters, will become ordered or will be eliminated by the formation of two- or three-dimensional defects such as dislocation loops,

shear planes, voids, etc. [30]. For the actinide oxides, the dominating defect species are often not the rate controlling factor for diffusion dependent processes. In the fluorite structure, cation mobility is many orders of magnitude smaller than anion mobility. At 1400 °C, D^O/D^U is found to be greater than 10^5 for UO_2 (depending on x) [31]. Cation diffusion coefficients are, therefore, difficult to measure.

Interdiffusion coefficient D in the ThO_2–PuO_2 system is expected to be strongly dependent on the oxygen potential, plutonium content and temperature like D in the UO_2–PuO_2 system [32]. It is well known that the tracer diffusion coefficient of U, i.e. D^U and of Pu, i.e. D^{Pu} in UO_{2+x} and MO_{2+x}, respectively vary by 4–5 orders of magnitude at constant temperature if the oxygen potential is varied [23,32]. Since hyperstoichiometric thorium oxide does not exist, the only possible deviation from stoichiometry for ThO_2–PuO_2 system is MO_{2-x}. The expected strong dependence of D^M on x in MO_{2-x} was confirmed by experiments on plutonium in MO_{2-x} [31]. Three possible mechanisms have been suggested for MO_{2-x} [23,30,31]. They are:

(a) vacancy mechanism, when $O/M > 1.98$,
(b) interstitial mechanism for a lower O/M ratios of $1.95 < O/M < 1.98$,
(c) cluster mechanism for $O/M < 1.95$.

5.2. Previous work on ThO_2–PuO_2

Paucity of data are available in the literature on the sintering in the ThO_2–PuO_2 system. Paprocki et al. [33] found that the sintering of PuO_2 and ThO_2 mixtures in Ar at around 1700 °C results in formation of solid solution. But the sintering in H_2 caused in reduction of PuO_2 to Pu_2O_3, which prevents from forming a homogeneous solid solution. Freshley and Mattys [11,12] investigated the sinterability, melting point and lattice parameters of PuO_2 and ThO_2 mixtures. The sintering studies showed that the sintered density of (Th, Pu)O_2 compacts increases with the increase in PuO_2 content between 2 and 50 at.%PuO_2 [34,35]. At concentrations greater than 50%PuO_2, the apparent density was lowered because of cracking [11]. The addition of a small amount of PuO_2 enhances the sinterability of ThO_2 in the same way as CaO. A sintered density of 96% TD was obtained at 1600 °C in H_2 atmosphere for ThO_2 containing 2–18% of PuO_2. The complete solid solution formation between ThO_2 and PuO_2 is reported in He at 1650 °C for 6 h. A minimum in sintered density was noticed for a composition corresponding to 50%PuO_2 when the sintering was carried out in the above atmosphere. Freshley and Mattys [11] also reported a linear decrease in lattice parameter with the increase in PuO_2 content of the mixture. The XRD pattern of PuO_2 rich pellets sintered in He revealed the existence of traces of α-Pu_2O_3. The low intensity peaks corresponding to β-Pu_2O_3 were also recorded.

5.3. Effect of dopant

Since ThO_2 is a very stable oxide, it can be sintered in various atmospheres such as air, H_2, Ar or vacuum. A sintering temperature as high as 2000 °C is required to attain about 80% TD with no additives. But with the addition of suitable additives the sintering proceeds at a temperature as low as 1150 °C in air [36]. Deviations from stoichiometry produce point defects. Similar effects can also be achieved by chemical doping of MgO/CaO to ThO_2. It is well known that the addition of aliovalent cations accelerates the sintering of ThO_2 [36]. The effect of an additive depends mainly on its valency. When the oxide of the metal which has a valency different from that of thorium is added to ThO_2, the following cases are possible to occur [26,36–38]:

1. Creation of vacancies/interstitials in Th sites.
2. Creation of oxygen interstitials/vacancies.
3. Increase/decrease of valency of some Th ions.
4. Decrease/increase of valency of some O ions.

Among the above possibilities, those cases prevail for which energy difference is the smallest. In the absence of a liquid phase, the additive may assist sintering by one of the two possible mechanisms [36]. Firstly, the additive may create point defects in the ThO_2 lattice and thereby increases the diffusion of Th^{4+} ion by many orders of magnitude. A typical example is seen for Nb_2O_5 in ThO_2. Secondly, the additive may significantly retard the grain growth so that pores are linked to the grain boundaries [38]. For example, addition of MgO to Al_2O_3 has been found to inhibit the grain growth or prevent discontinuous grain growth. The additive inhibits boundary migration by a solute drag mechanism and retains the pores at the grain boundaries [38]. This is the case of MgO/CaO in ThO_2. The effect of higher valency additive is seen to be the same as that of higher oxygen pressure in the atmosphere. If an oxidizing atmosphere is used along with a higher valency additive, the effect is added up. If an oxidizing atmosphere is used with a lower valency additive, the effects nullify each other. When the range of stoichiometry is large as found in UO_2, advantage is taken by increasing the oxygen pressure in the sintering atmosphere. When the range of stoichiometry is small as found in ThO_2 advantage is taken by introducing additives [36–38]. While choosing an atmosphere or additive for achieving activated sintering, it should be remembered that the effect of one must add to the other.

Balakrishna et al. [36] demonstrated that ThO_2 could be sintered to densities greater than 9.76 g/cm^3 at 1150 °C by doping with 0.25 mol%Nb_2O_5. Ananthasivan et al. [39]

have shown that the effect of higher valence additives, viz., V, Nb and Ta through gel-combustion synthesis on the densification of ThO_2. Nair et al. [40] reported that MgO, CaO, and Nb_2O_5 bring about accelerated sintering in ThO_2. Among the pentavalent dopants, 0.5 mol%Nb_2O_5 is the most effective in bringing about the accelerated sintering in ThO_2. EPMA examination of pellets doped with Nb_2O_5 revealed that the amount of niobium present in the various regions of the pellets was below the detection limit suggesting a homogeneous distribution of niobium in the sintered pellets. The microstructure of the pellet sintered at 1350 °C showed enlarged grain boundaries, suggesting the onset of melting [39]. Ananthasivan et al. [39] have reported the existence of a eutectic isotherm in the Nb_2O_5–ThO_2 system at 1333 °C for 27 mol%Nb_2O_5. Hence a temperature as high as 1333 °C is necessary in order to bring about liqudation in ThO_2 doped with Nb_2O_5.

With the above background in mind, we will discuss the effect of various atmospheres and dopants on the shrinkage behaviour of the ThO_2–PuO_2 pellets.

5.4. Effect of CaO

In ThO_2, the diffusion of Th^{4+} ions is many times lower than that of O^{2-} ions. The addition of lower valency additives like MgO or CaO to ThO_2 is expected to create vacant oxygen sites in ThO_2 lattice. ThO_2 is always stoichiometric unless deviations from stoichiometry are produced chemically, e.g., by adding CaO to produce oxygen deficient (Th, Ca)O_{2-x} [23]. Such materials produce one oxygen vacancy per added impurity atom due to the charge neutrality condition.

The addition CaO to ThO_2 creates defects since calcium has a lower valency than thorium. Theoretically, there are two possible types of defects to be formed, i.e. oxygen vacancies and metal interstitials. The reducing atmosphere further reinforces the formation of such defects. Hence a lower valency additive and a reducing atmosphere will give a synergetic effect. In the PuO_2–ThO_2 system, both Th^{4+} and Pu^{4+} ions may be replaced by Ca^{2+} ions. As mentioned above, this will lead to the generation of defects. Since the energy to form an oxygen vacancy is much lower than that to form a metal interstitial in the fluorite type oxides, most defects are formed as a result of calcium substitution will be the oxygen vacancies. The metal interstitials are also formed together at that time, but their amount is very small compared with that of oxygen vacancies. But metal diffusion is supposed to take place via such metal vacancies. That is to say, the metal diffusion will be enhanced by the addition of CaO. However in reducing atmosphere, Th^{4+} ions remain unaffected, but some of the Pu^{4+} ions are reduced to Pu^{3+} ions. The formation of Pu^{3+} ions is accompanied by the generation of metal interstitials. From Fig. 8, it can be seen that the shrinkage is faster in CaO doped ThO_2–75%PuO_2 compared with ThO_2–30%PuO_2 and ThO_2–50%PuO_2 pellets. The XRD data of this pellet indicate the presence of two phases. The larger sintering of ThO_2–75%PuO_2 in Ar–8%H_2 observed in this study may be associated with the presence of defect structure as a proportion of the PuO_2 gets reduced to Pu_2O_3. This has been confirmed by XRD analysis. The migration energies of Pu^{3+} and Pu^{4+} ions are 4.11 and 5.95 eV, respectively [32] (see Table 5). The Pu^{3+} ions can move faster than Pu^{4+} ions resulting in faster diffusion. Therefore, the formation of Pu_2O_3 in the sample helps in achieving a faster shrinkage rate [41]. ThO_2–75%PuO_2 sinters well also in Ar too because at high temperature PuO_2 loses its stoichiometry and becomes PuO_{2-x}. This defect structure enhances the sintering of PuO_2 pellets. Our results have been found to agree with the earlier observations reported on PuO_2 [41].

Table 5
Ionic radii and migration energies of Th, Pu and U ions

	Ionic radius (nm)	Migration energy (eV)
U^{4+}	0.097	6.0
Th^{4+}	0.102	–
Pu^{3+}	0.108	4.11
Pu^{4+}	0.093	5.95

5.5. Effect of Nb_2O_5

When one Th^{4+} ion is substituted by one Nb^{5+} ion in the ThO_2 lattice, the effective positive charge of 1+ is imparted on the lattice. Hence the addition of Nb_2O_5 to ThO_2 causes to form significantly high concentrations of oxygen interstitial ions. Metal vacancies will also be formed at the same time but in very low concentrations. An increase in thorium lattice vacancy, increases its diffusion coefficient. If sintering is carried out in H_2, sintering aid cation (Nb^{5+}) is expected to be reduced. If these reduced cations were to replace the Th^{4+} ions substitutionally, an increase in oxygen lattice vacancy should be expected, leading to a lower Th-ion Schottky vacancy equilibrium concentration, which will result in a decrease in Th diffusivity [36,42]. Thus Nb_2O_5 will not be much useful in reducing atmosphere.

In the ThO_2–PuO_2 system, Nb^{5+} ions substitute for both Th^{4+} and Pu^{4+} ions thereby increasing the concentration of cation vacancies. When the sintering has been carried out in Ar and Ar–8%H_2, the valence of thorium remains Th^{4+} since this state is the only stable valence state of thorium. But some of the Pu^{4+} ions will be reduced especially in Ar–8%H_2 to Pu^{3+} ions at high temperatures. Hence the creation of Pu^{3+} ions in the oxide should enhance the sintering since more cation vacancies are generated by the above process. However,

in the reducing atmosphere like Ar–8%H_2, Nb_2O_5 is also reduced to lower oxides: $Nb_2O_5 \rightarrow NbO_2 \rightarrow Nb_2O_3 \rightarrow NbO$ [36,43]. This means that niobium acts as a lower valency additive to ThO_2 in a reducing atmosphere. Its behaviour will become then similar to CaO and hence sintering should be enhanced. Our results have shown that in both Ar and Ar–8%H_2, shrinkage was found to be high for CaO doped pellets for all the metal ratios covered in this study. Even at 1650 °C, the shrinkage was only for 6% for ThO_2 doped with Nb_2O_5 pellet but it was 12% for the CaO doped pellet of the same $Pu/(Pu + Th)$ ratio (see Fig. 2). Balakrisna et al. [36] reported that a high sintered density of 97% can be achieved in $ThO_2 + Nb_2O_5$ pellets in reducing atmosphere at 1700 °C. The reason that such a high density could not be obtained in this study may be because all the Nb_2O_5 might not have been reduced to the lowermost valency state and thus existing in mixed valency states.

In conclusion it can be said that the addition of a higher valency additive is best for an oxidizing atmosphere for enhanced sintering. It is reported that in air the Nb_2O_5 doped pellet needs a sintering temperature of only 1150 °C. But in reducing atmosphere much higher sintering temperature (1700 °C) is required to attain the same density. It suggests that Nb_2O_5 is a more effective dopant in oxidative atmosphere than in reducing atmosphere [38]. This can be explained from the electrical conductivity measurements carried out on ThO_2 by Bransky and Tallan [44]. They noticed that in the oxidizing region, the increase in electrical conductivity occurred in both low and high temperatures. However, in the reducing atmosphere the increase in electrical conductivity was observed only at higher temperatures. Thus at low temperatures the combination of higher valency additive and oxidizing atmosphere leads to give a higher defect concentration than does the combination of lower valency additive and reducing atmosphere [45].

5.6. Effect of PuO_2

From Figs. 2–8, it is clear that the addition of PuO_2 to ThO_2 enhances sintering for both CaO and Nb_2O_5 doped pellets. The PuO_2 powder used in these experiments has a higher BET surface area than ThO_2 (see Table 1). Hence, PuO_2 is expected to sinter more readily than ThO_2. Pritchard and Nance [46] have studied the sintering behaviour of PuO_2 in different atmospheres. PuO_2 has been found to sinter largely in H_2 than in Ar. Chikalla et al. [47] have reported that PuO_2 can be reduced to ~50%α-Pu_2O_3 on heating in H_2 at 1650 °C or to 25%Pu_2O_3 on just heating at 1450 °C. PuO_2 loses little amount oxygen on heating at 1100–1200 °C in inert or reducing atmosphere but loses oxygen readily at high temperature [48,49]. The oxygen deficiency results in formation of Pu^{3+} ion which helps in enhancing sintering. Pu^{3+} ions were shown to diffuse faster in ThO_2 than Pu^{4+} ions. Therefore formation of Pu_2O_3 in the sample helps in achieving a faster shrinkage rate [49]. The superior sintering behaviour of ThO_2–PuO_2 in Ar–8%H_2 observed in this study may be associated with the presence of defects which are formed when PuO_2 is partly reduced to Pu_2O_3. This has been confirmed by XRD analysis. PuO_2 sinters well in Ar because at high temperature PuO_2 loses its oxygen forming PuO_{2-x}. This defect enhances the sintering. Our results have been found to agree with the earlier observations reported on PuO_2 [49].

5.7. Effect of atmosphere

Our study has shown that shrinkage is marginally larger in Ar–8%H_2 than that in Ar for temperatures greater than 1000 °C for all the metal ratios except for Nb_2O_5 doped ThO_2–75%PuO_2. The similar observation has also been made for the UO_2–PuO_2 system by the same authors [48].

Another important point noticed during the densification is the retardation of shrinkage at around 1000 °C in Ar and Ar–8%H_2 for ThO_2–50%PuO_2 and ThO_2–75%PuO_2. The retardation of shrinkage correlates with the onset of the solid solution formation. The solid solution is formed by the interdiffusion of Pu^{4+} ion into ThO_2 lattice and Th^{4+} ion into PuO_2 lattice. This interdiffusion process decreases the sintering rate and shifts the shrinkage to a higher temperature. Such phenomenon has been reported for UO_2–PuO_2 and UO_2–Gd_2O_3 fuels [50,51].

The formation of Pu_2O_3 during the sintering results in expansion of the unit cell. The ionic radii of Pu^{3+} and Pu^{4+} ions are 0.108 and 0.093 nm, respectively (Table 5). Thus the expansion in the shrinkage curves at around 900–1100 °C (see Fig. 8) may be attributed to the formation of large Pu^{3+} ion [23,32].

As mentioned before, the larger sintering of ThO_2–PuO_2 pellets in Ar–8%H_2 observed in this study may be associated with the presence of defects as PuO_2 is reduced to Pu_2O_3.

5.8. Low temperature behaviour of ThO_2

During the sintering of ThO_2, a prominent peak was observed in the shrinkage curve at around 100–300 °C (see Fig. 2). This peak was observed only for ThO_2 and was seen for both the dopants of CaO and Nb_2O_5 and for both the atmospheres. The formation of peak in ThO_2 may be explained from the following points:

1. The green density of pure ThO_2 was the highest around 67%. The green density was found to decrease with the increase of PuO_2 content.

2. The ThO_2 pellets were prepared by using zinc behenate binder. The binder usually volatilizes off at low temperature in the range of 150–250 °C.

The green density depends on the compatibility characteristics of the starting ThO_2/PuO_2 powder. The flowability of the powder depends upon its shape and its resistance to form interlocks. In our case the characteristics and morphologies of the powder are such that at the same compaction pressure ThO_2 powder will compact to a higher density than that of PuO_2. Therefore, the green density of ThO_2–PuO_2 compacts decreases with the increase of PuO_2 content.

When the ThO_2 pellets of high green density are heated in a dilatometer, the gases trapped in the porosity cannot easily to escape. The pressure of such gases in the porosities increases on heating, which causes the pellet to bulge a little. On further heating to around 300 °C, the pressure inside the porosities causes some of the interconnected closed porosities to open up to the surface. This will lead to escape the gases resulting in the shrinkage of the pellet. Since ThO_2–PuO_2 pellets have comparatively low green density similar to UO_2 [52], there are a sufficient number of the interconnected channels in these pellets from the first, through which the trapped gases escape. Hence no peaks were found for these pellets.

To understand the effect of binder on the formation of peak, a few ThO_2 pellets were prepared without binder and compacted to the same green density. Dilatometric experiment was repeated with these pellets and it was found that peaks appeared again for the above pellets at around 100–300 °C. This result shows that the binder has not contributed to the formation of peaks for ThO_2 pellets. The peak observed for ThO_2 pellet in the temperature range of 100–300 °C is confirmed to be due to its high green density.

6. Conclusions

The shrinkage behaviour of ThO_2–PuO_2 compacts containing different amounts of PuO_2 was studied in Ar and Ar–8%H_2, and the following conclusions are drawn:

1. Out of the two dopants studied (CaO and Nb_2O_5), CaO was found to be more effective for sintering for all $Pu/(Pu + Th)$ ratios covered in this study.
2. ThO_2–50%PuO_2 and ThO_2–75%PuO_2 showed two phased structure and their shrinkage curve showed changes in slope in both Ar and Ar–8%H_2 at ~1100 °C.
3. Addition of PuO_2 to ThO_2 enhances sintering. This was found to be true for both the CaO and Nb_2O_5 dopants of the concentrations used in this study.
4. During the sintering of ThO_2, a prominent peak was observed in the shrinkage curve at around 100–300 °C. This peak is attributed to the pressure increase of trapped gases and their subsequent release at high temperatures.

Acknowledgements

The authors are grateful to Dr C. Ganguly, Chief Executive, Nuclear Fuels Complex, Hyderabad for his keen support and constant encouragement during the course of this work. They are also thankful to Messers T. Jarvis, K. Ravi, P. Sankaran Kutty, G.P. Mishra and S.K. Pal for their valuable support.

References

[1] F. Vettraino, G. Magnani, T. La Torretta, E. Marmo, S. Coelli, L. Luzzi, P. Ossi, G. Zappa, J. Nucl. Mater. 274 (1999) 23.
[2] N.L. Shapiro, in: Proceedings of Japan–US Seminar on Th Fuel Reactors, October 18–22, 1982, Nara, Japan, The Atomic Energy Society of Japan, 1985, p. 171.
[3] J. Magill, P. Peerani, Hj. Matzke, J. Van Geel, in: IAEA Technical Committee Meeting on Advanced Fuels with Reduced Actinide Generation, 21–23 November 1995, Vienna.
[4] C. Rubbia, S. Buono, E. Gonzalez, Y. Kadi, J.A. Rubio, European Organization for Nuclear Research, CERN/AT/95-53(ET), 12 December 1995.
[5] H.A. Feiveson, S.N. Rodionov, Science and Global Security 6 (1997) 265.
[6] C. Ganguly, in: M. Srinivasan, I. Kimura (Eds), Proceedings of Indo Japan Seminar of Th Utilization, December 10–13, 1990, Bombay, Indian Nuclear Society and the Atomic Energy Society of Japan, p. 77.
[7] T. Haga, in: Proceedings of Japan–US Seminar on Th Fuel Reactors, 18–22 October 1982, The Atomic Energy Society of Japan, Nara, Japan, 1985, p. 205.
[8] P. Rodriguez, C.V. Sundaram, J. Nucl. Mater. 100 (1981) 227.
[9] J. Magill, Hj. Matzke, G. Nicolaou, P. Peerani, J. Van Geel, in: Technical Committee Meeting on Recycling of Plutonium and Uranium in Water Reactor Fuel (IAEA), Newby Bridge, Windermere, UK 3–7 July 1995.
[10] J. Magill, P. Peerani, J. Van Geel, in: Second International ARS Topical Meeting on Advanced Reactor Safety, Orlando FL, 1–4 June, 1997.
[11] M.D. Freshley, H.M. Mattys, Hanford Power Products Division, Richland, Washington, HW-76300, 1962.
[12] M.D. Freshley, H.M. Mattys, Hanford Power Products Division, Richland, Washington, HW-76302, 1963.
[13] Gmelin Handbook der Anorgnischen Chemie, 8th Ed., Thorium, Springer Verlag, Berlin, Suppl. vols. C1 and C2.
[14] K. Bakker, E.H.P. Cordfunke, R.J.M. Konings, R.P.C. Schram, J. Nucl. Mater. 250 (1997) 1.
[15] R.N.R. Mulford, F.H. Ellinger, J. Phys. Chem. 62 (1958) 1466.

[16] J.K. Dawson, J. Chem. Soc. (1952) 1882.
[17] M.H. Rand, in: Thorium: Physico-chemical Properties of its Compounds and Alloys, Atomic Energy Review, Special Issue No. 5, IAEA, Vienna, 1975 p. 7.
[18] H.A. Wriedt, Bull. Alloy Phase Diagram 11 (1990) 184.
[19] T.M. Besmann, J. Nucl. Mater. 144 (1987) 141.
[20] T.D. Chikalla, C.E. Mcneilly, R.E. Skavdahl, Hanford atomic production operation report, Richland, Washington, HW-74802, 1962.
[21] E.R. Gardner, T.L. Markin, R.S. Street, J. Inorg. Nucl. Chem. 27 (1965) 541.
[22] Hj. Matzke, Philos. Mag. 64A (1991) 1181.
[23] Hj. Matzke, in: T. Sorensen (Ed.), Non-stoichiometric Oxides, Academic Press, New York, 1981, p. 156.
[24] C.R.A. Catlow, J. Chem. Soc. Faraday Trans. 2 (83) (1987) 1065.
[25] E.E. Jackson, M.H. Rand, Atomic energy research establishment, Harwell Report, AERE-R-3636, 1960.
[26] D.R. Olander, Fundamental aspects of nuclear reactor fuel elements, TID-26711-P1, US Department of Energy, 1976, p.145.
[27] R.N.R. Mulford, F.H. Ellinger, J. Am. Chem. Soc. 80 (1958) 2023.
[28] Hj. Matzke, AECL Report, AECL-2585, 1966.
[29] A.B. Lidiard, J. Nucl. Mater. 19 (1966) 106.
[30] G.E. Murch, C.A. Catlow, J. Chem. Soc. Faradays Trans. 2 (83) (1987) 1157.
[31] Hj. Matzke, J. Phys. 34 (1973) 317.
[32] Hj. Matzke, J. Chem. Soc. Faradays Trans. 2 (86) (1990) 1243.
[33] S.J. Paprocki, D.L. Keller, W.M. Pardue, in: Properties of PuO_2 and PuO_2–ThO_2 Ceramics, USAEC Report APEX-696, Nuclear Materials and Propulsion Operation, General Electric, October, 1961.
[34] A.T. Jeffs, Trans. Am. Nucl. Soc. 11 (1968) 497.
[35] D.E. Ramissen, M.W. Benecke, W.R. Jentzen, R.B. McCord, Trans. Am. Nucl. Soc. 32 (1979) 246.
[36] P. Balakrishna, B.P. Varma, T.S. Krishnan, T.R.R. Mohan, P. Ramakrishnan, J. Nucl. Mater. 160 (1988) 88.
[37] K.C. Radford, J.M. Pope, J. Nucl. Mater. 116 (1983) 305.
[38] P. Balakrishna, in: Sintering of Uranium Dioxide: An Introduction, Nuclear Fuels Complex, Hyderabad, 1987, p. 28.
[39] K. Ananthasivan, S. Anthonysami, C. Sudha, A.L.E. Terrance, P.R. Vasudeva Rao, J. Nucl. Mater. 300 (2002) 217.
[40] M.R. Nair, U. Basak, R. Ramachandran, S. Majumdar, Trans. Powder. Met. Assoc. India 26 (1999) 53.
[41] T.R.G. Kutty, P.V. Hegde, R. Keswani, K.B. Khan, S. Majumdar, D.S.C. Purushotham, J. Nucl. Mater. 264 (1999) 10.
[42] P. Balakrishna, G.V.S.R.K. Somauajulu, T.S. Krishnan, T.R.R. Mohan, P. Ramakrishnan, in: P. Vincenzini (Ed.), Ceramics Today–Tomorrow's Ceramics, Elsevier, Amsterdam, Netherlands, 1991, p. 2995.
[43] P. Balakrishna, B.P. Varma, T.S. Krishnan, T.R.R. Mohan, P. Ramakrishnan, J. Mater. Sci. Lett. 1 (1988) 657.
[44] I. Bransky, N.M. Tallan, J. Am. Ceram. Soc. 53 (1970) 625.
[45] D.D. Upadhyaya, C.M. Sunta, J. Nucl. Mater 127 (1985) 137.
[46] W.C. Pritchard, R.L. Nance, Los Alamos Report, Los Alamos, LA-3493, 1965.
[47] T.D. Chikalla, C.E. McNeilly, R.E. Skavdahl, J. Nucl. Mater. 12 (1964) 131.
[48] T.R.G. Kutty, P.V. Hegde, K.B. Khan, S. Majumdar, D.S.C. Purushotham, J. Nucl. Mater. 281 (2000) 10.
[49] T.R.G. Kutty, K.B. Khan, P.V. Hegde, A.K. Sengupta, S. Majumdar, D.S.C. Purushotham, J. Nucl. Mater. 297 (2001) 120.
[50] R. Manzel, W.D. Dorr, Bull. Am. Ceram. Soc. 59 (1980) 601.
[51] W. Dorr, S. Hellmann, G. Mages, J. Nucl. Mater. 140 (1986) 7.
[52] T.R.G. Kutty, P.V. Hegde, K.B. Khan, S.N. Pillai, A.K. Sengupta, G.C. Jain, S. Majumdar, H.S. Kamath, D.S.C. Purushotham, J. Nucl. Mater. 305 (2002) 159.